



A New Cu(II) Complex of PAMAM Dendrimer Modified with 1,8-Naphthalimide: Antibacterial and Anticancer Activity

Hristo Manov¹, Desislava Staneva², Evgenia Vasileva-Tonkova³ , Radostina Alexandrova⁴, Radostina Stoyanova⁵, Rositka Kukeva⁵, Stanimir Stoyanov¹, Ivo Grabchev^{6,*} 

¹ Sofia University "St. Kliment Ohridski", Faculty of Chemistry and Pharmacy, 1187 Sofia, Bulgaria

² University of Chemical Technology and Metallurgy, 1756 Sofia, Bulgaria

³ The Stephan Angeloff Institute of Microbiology, Bulgarian Academy of Sciences, 1113 Sofia, Bulgaria; evaston@yahoo.com (E.V.T);

⁴ Institute of Experimental Morphology, Pathology, and Anthropology with Museum, Bulgarian Academy of Sciences, Acad. G. Bonchev Street, Bl. 25, 1113 Sofia, Bulgaria

⁵ Institute of General and Inorganic Chemistry, Bulgarian Academy of Sciences, 1113 Sofia, Bulgaria

⁶ Sofia University "St. Kliment Ohridski", Faculty of Medicine, 1407 Sofia, Bulgaria

* Correspondence: i.grabchev@chem.uni-sofia.bg (I.G.);

Scopus Author ID 7004847951

Received: 6.07.2021; Revised: 22.08.2021; Accepted: 26.08.2021; Published: 19.10.2021

Abstract: A new fluorescent PAMAM copper complex ($[Cu_2(D)(NO_3)_4]$) has been synthesized and identified. The formation of the complex has been investigated by fluorescence spectroscopy which revealed two copper ions to be bound to the dendrimer ligand. That has also been confirmed upon subjecting the solid copper complex to electron paramagnetic spectroscopy. The antimicrobial activity of the copper complex against Gram-negative bacterium *Pseudomonas aeruginosa* in light and the dark has been studied. The results demonstrate an increase in its activity when irradiated with daylight. This activity of the copper complex is retained even after being loaded onto a cotton cloth. The antitumor activity of the copper complex and dendrimer ligand against triple-negative breast cancer MDA-MB-231 cells has been investigated as well.

Keywords: metallodendrimers; 1,8-naphthalimide; antimicrobial activity; antitumor activity; antibacterial textile

© 2021 by the authors. This article is an open-access article distributed under the terms and conditions of the Creative Commons Attribution (CC BY) license (<https://creativecommons.org/licenses/by/4.0/>).

1. Introduction

With the development of synthetic organic chemistry, new opportunities have been created to develop and study novel three-dimensional macromolecules, the so-called dendrimers. They are characterized by monodispersity and perfectly branched symmetrical structure. Combining the properties of low- and high molecular substances, dendrimers have been enjoying a constantly growing interest [1-4].

There are a number of examples of successful use of dendrimers as ligands for the production of metallodendrimers, which have demonstrated very good microbiological and antitumor activity [5-7]. Biologically important metal ions such as Cu(II), Co(II), Zn(II), Fe(II), Fe(III) play a key role in the structural organization of enzymes and biologically active substances in living organisms. Therefore, in recent years, much research has been focused on preparing metal complexes with different organic ligands, aiming to improve existing

chemotherapeutics' action [8-10]. The design, synthesis, and study of new ligands and their metal complexes are of interest as their biological activity depends on the nature of metal ions and the chemical structure of the ligands and the type of bond occurring between them.

Fluorescent dendrimers containing chromophore fragments at specific, predetermined positions of the molecule have been developed. The tailoring has yielded new properties and new areas of their application in chemistry, biology, pharmacy, nanomedicine, and others. Modification of PAMAM and PPA dendrimers with organic fluorophores such as 1,8-naphthalimide [11,12], rhodamine [13], benzanthrene [14], acridine [15], 4-nitrobenzofurazan [16], curcumin [17] results in obtaining fluorescent dendrimers with very good photophysical characteristics. Our laboratory has been carrying out targeted research to elucidate the structure-property relationship of such photoactive dendrimers. Our previous research has shown, on the one hand, that such dendrimers can be used to detect metal ions and protons [11], and on the other hand, that they exhibit good antimicrobial [15,16,18-21] and antitumor activity [22].

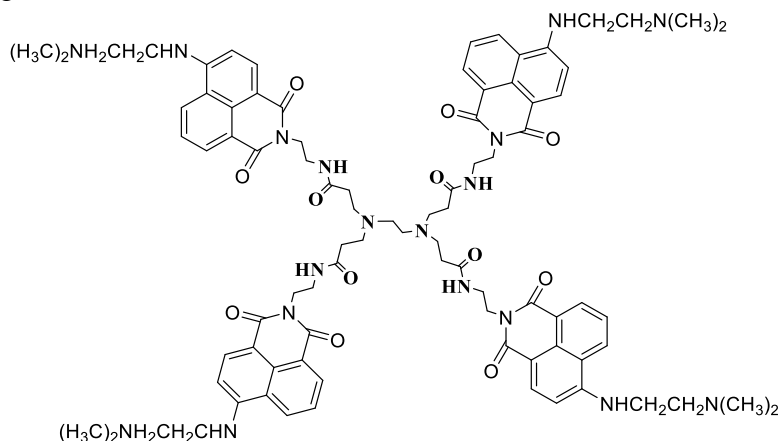
Among the known fluorophores with well-defined biological activity, an important place is occupied by 4-substituted 1,8-naphthalimides due to the ability of 1,8-naphthalimide derivatives to interact with different biological systems through non-covalent interactions, such as π - π stacking. Hence, the wide biomedical interest in these compounds of high antitumor, antimicrobial, antiviral or anti-inflammatory activity [23-26].

Moreover, dendrimer molecules have a large number of closely related functional groups in their structure. If these groups are functionalized with biologically active substances, one can expect the dendrimer molecule to enhance its biological activity compared to that of low molecular weight compounds.

This study presents the synthesis and characterization of a new zero-generation polyamidoamine (PAMAM) dendrimer-based metallodendrimer modified with four 1,8-naphthalimide fragments. Its antibacterial activity has been examined in the dark and upon irradiation with daylight. The experiments have been carried in solution and when loaded onto cotton fabric. The antitumor activity of the new metallodendrimer against triple-negative breast cancer MDA-MB-231 cells has also been studied.

2. Materials and Methods

The synthesis and the characterization of dendrimer D used as a ligand in this study were already described [27]. All methods used for the analysis and investigations are described in the Supporting information.



Scheme 1. Chemical structure of dendrimer D.

2.1. Synthesis of Cu(II) complex of dendrimer D: $[Cu_2(D)(NO_3)_4]$.

Dendrimer D (1.580g, 0.001M) was dissolved in ethanol, and copper nitrite (0.751g, 0.004M) was added under reflux. The reaction mixture was stirred for 3 hours. After cooling, the precipitate formed was filtered off, washed three times with 10 ml of ethanol, and dried.

Yield: (1.68g, 86%)

FTIR: cm^{-1} : 2928, 2854, 1635, 1581, 1547, 1419, 1395, 1340, 1241, 1183, 1035, 774, 757, 579, 498,

Analysis: $C_{86}H_{104}O_{24}N_{22}Cu_2$ (1955.2 g/mol): Calcd C 52.78, H 5.32, N 15.75; Found C 52.89, H 5.40, N 15.78.

2.2. Treatment of the cotton fabric with dendrimer D and $[Cu_2(D)(NO_3)_4]$.

A piece of cotton fabric (140 g/m^2) weighing 1 g was added to 10 ml of DMF solution of dendrimer D (2.50 mg) and its Cu (II) complex at 40°C. After 60 min, the cotton sample was washed with distilled water and dried at room temperature. Fluorescent spectroscopy measurements showed that 2.2mg of (D) and 2.1mg of (copper complex) had been loaded onto the cotton surface.

3. Results and Discussion

3.1. Chemical investigations.

The synthesis of dendrimer D used as a ligand has been described previously [27]. The substituent at the C-4 position of the 1,8-naphthalimide fluorophore structure $-NH-CH_2CH_2(NCH_3)_2$ has been tailored to act as a receptor fragment in the formation of various biologically active metal complexes - such as Cu (II) Zn (II), Co (II), Fe (II), Fe (III) complexes, etc. Its main photophysical characteristics have been studied in organic solvents of different polarities. It has been shown that in non-polar media, the quantum efficiency of this dendrimer is much better expressed if compared to that in non-polar solvents [28]. In the presence of metal ions, the fluorescent intensity of dendrimer D is amplified several times, which is due to the quenching of the photoinduced electron transfer occurring from the distant nitrogen atom ($-N(CH_3)_2$) to the fluorophore 1,8-naphthalimide system [29].

Studies have been performed to evaluate the effect that the concentration of Cu (II) ions has on the fluorescence intensity of dendrimer D. DMF has been used as a solvent since dendrimer D has a low fluorescence intensity (FF = 0.11) [28]. On the other hand, copper nitrate dissolves very well in it, so does the copper complex formed. The fluorescence spectra of dendrimer D during its titration with Cu (II) ions in a concentration range up to 2.5×10^{-5} M is plotted in Figure 1A. The results show that the fluorescence intensity increases in proportion to the concentration of Cu (II) ions (Figure 1B), and saturation is reached at a 1:2 ratio between the dendrimer and copper complex Cu(II) ions. That illustrates how both Cu(II) ions from a complex with dendrimer D. As seen from Figure 1A, the position of the fluorescence spectrum does not change during the complex formation. That means the copper ions form a coordinate bond with the distant nitrogen atom ($-N(CH_3)_2$) of the 1,8-naphthalimide structure, where one copper ion coordinates with two 1,8-naphthalimide fragments, as shown in Scheme 2. In this case, the ratio between the dendrimer and Cu (II) ions is 1:2.

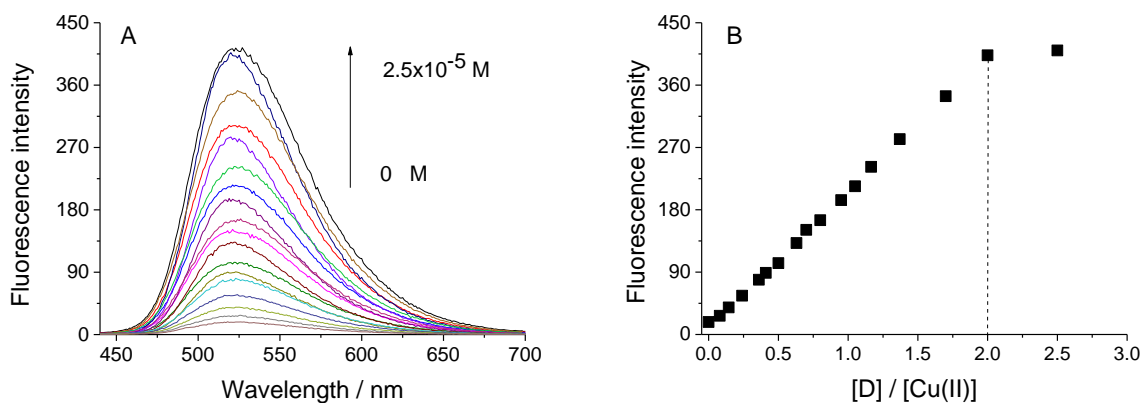
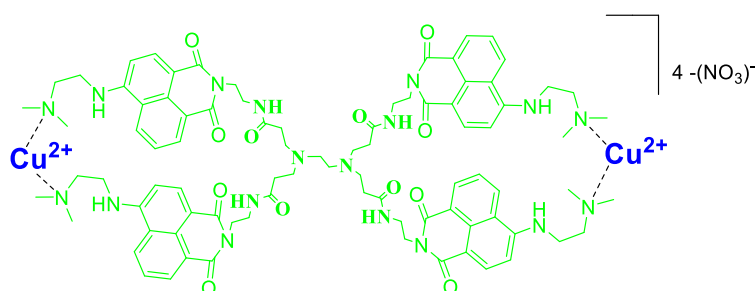


Figure 1. (A) Fluorescence spectra of dendrimer D in DMF solution ($c = 1 \times 10^{-5}$ M) at different concentrations of Cu(II) cations (from 0 to 2.5×10^{-5} M); (B) Dependence of the fluorescent intensity on the concentration of Cu (II) ions.



Scheme 2. Proposed structure of the complex of dendrimer D with Cu (II) ions $[\text{Cu}_2(\text{D})(\text{NO}_3)_4]$.

3.2. EPR investigations.

The EPR spectrum of Cu (II) ions coordinated by dendrimer ligand D displays an anisotropic signal with the g -components of $g_{\parallel}=2.259$ and $g_{\perp}=2.030$, and a hyperfine constant of $A_{\parallel}=16.5$ mT. The g - and A -components remain constant in the temperature range of 100 – 295 K. These EPR parameters are typical for Cu (II) ions located in a tetragonally elongated crystal field. The magnitude of the g_{\parallel} -component is relatively low, while the constant hyperfine A_{\parallel} possess a relatively high value. Considering the Peisach – Blumberg diagram [30] of the relation between the values of g - and A -components, it appears that Cu (II) ions are, most probably, coordinated through N and O atoms. Furthermore, the EPR spectrum allows evaluating the ratio between Cu (II) and dendrimer ligand D. The calculation shows that two Cu(II) ions are attached to one dendrimer ligand.

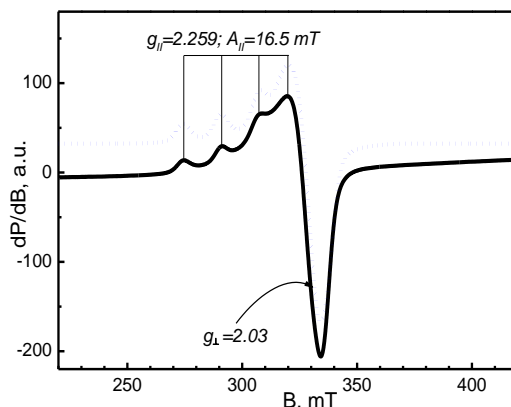


Figure 2. EPR spectrum of the complex between Cu (II) and D-ligand taken at 100 K. The blue line corresponds to the simulated spectrum.

3.3. Colorimetric characteristics of cotton fabrics treated with dendrimers D and [Cu₂(D)(NO₃)₄].

In order to obtain antibacterial textiles, 100% cotton fabrics have been treated with dendrimer D and its copper complex [Cu₂(D)(NO₃)₄]. The color characterization of the cotton fabrics has been conducted by determining the CIEab parameters (L*, a*, and b*) and the respective chromaticity coordinates (x and y). The fabrics have been evaluated quantitatively and qualitatively by the corresponding color coordinates L*, a*, b*, (equations 1-3):

$$L^* = 116 (Y/Y_0)^{1/3} - 16 \tag{1}$$

$$a^* = 500 [(X/X_0)^{1/3} - (Y/Y_0)^{1/3}] \tag{2}$$

$$b^* = 200 [(Y/Y_0)^{1/3} - (Z/Z_0)^{1/3}] \tag{3}$$

where, X₀, Y₀, Z₀ are the tristimulus values of specified achromatic light used for illuminating the untreated color fabrics, while X, Y, Z are the values for the colored fabrics, respectively. The value of Y₀ has been normalized in such a way that Y₀ = 100. The color characteristics of the dyed cotton fabric treated with dendrimers are summarised in Table 1. The results show that, the dyed cotton fabrics have a yellow color. In the case of using metallodendrimer [Cu₂(D)(NO₃)₄], the cotton fabric obtains a yellow color deeper than the one of the cotton fabric treated with D. The color difference ΔE* has been calculated according to equation 4. These values have been used for the quantitative determination of color [31].

$$\Delta E^* = [(\Delta L^*)^2 + (\Delta a^*)^2 + (\Delta b^*)^2]^{1/2} \tag{4}$$

, where ΔL*, Δa*, Δb* are the difference in the coordinates of the control cotton fabric and of respective cotton fabrics treated with dendrimer D and [Cu₂(D)(NO₃)₄], respectively. The value of the untreated cotton fabric is ΔE* = 0. The results show that, when loading the fabric with the metallodendrimer, the color saturation achieved (ΔE* = 39.247) is better than the yielding when dendrimer D (ΔE* = 34.791) is used.

Table 1. Color characteristics of treated with dendrimers D and [Cu₂(D)(NO₃)₄] cotton fabric.

Cotton samples	L*	a*	b*	X	Y	Z	x	y
Cotton	93.77	-0.26	3.75	80.22	84.75	85.65	0.3201	0.3382
Cotton +D	92.81	-7.44	37.78	74.58	82.45	45.11	0.3688	0.4081
Cotton + [Cu ₂ (D)(NO ₃) ₄]	95.82	-11.39	41.33	79.00	89.53	46.58	0.3673	0.4162

3.4. Biological investigations.

3.4.1. Antimicrobial activity.

The effect of light on the antimicrobial activity of the investigated [Cu₂(D)(NO₃)₄] against Gram-negative bacteria *P. aeruginosa* has been tested by the broth dilution test. The experiments were conducted in a planktonic format in solution and applied on cotton fabric. The microbial growth decreases with the increasing concentration of [Cu₂(D)(NO₃)₄] in the presence of light and the dark. Under light irradiation, it is lower than in the dark, which indicates higher antimicrobial activity (Figure 3). The higher antimicrobial activity of the studied photoactive dendrimer under light irradiation can be explained by its ability to bind to the bacterial membrane and generate reactive oxygen upon photostimulation [32].

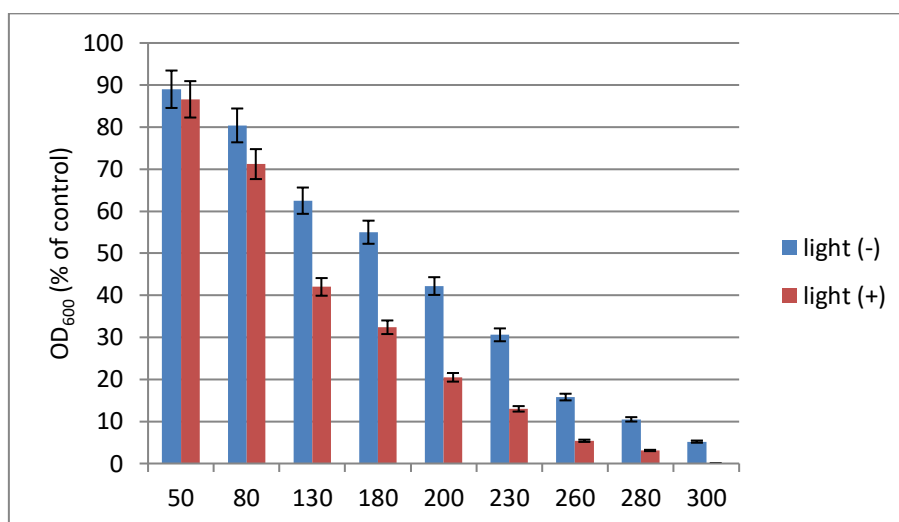


Figure 3. Growth (expressed by OD₆₀₀) of *P. aeruginosa* at different concentrations of [Cu₂(D)(NO₃)₄] under light irradiation and in the dark.

3.4.2. Antimicrobial activity of modified cotton fabric.

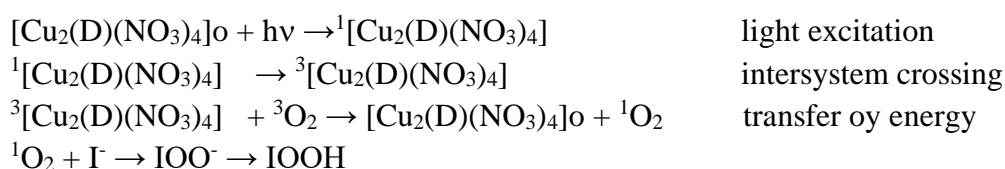
The antimicrobial effect of the cotton fabric treated with [Cu₂(D)(NO₃)₄] has been tested in nutrient broth by reducing the growth of *P. aeruginosa* as a model strain. The results reveal that the presence of light cotton fabric treated with [Cu₂(D)(NO₃)₄] inhibits microbial growth by about 22% and by about 14% in the dark. Metallodendrimer [Cu₂(D)(NO₃)₄] is being attached to the cotton surface mainly by hydrogen bonds and Van der Waals interactions. It is hypothesized that the direct contact of bacterial cells with cotton surfaces contributes to the antimicrobial effect of the treated cotton fabric. The low water solubility of [Cu₂(D)(NO₃)₄] does not allow the easy release of bacterial cells from the cotton surface to contact directly with bacterial cells in solution. That explains the low growth inhibition of the tested bacteria in the solution.

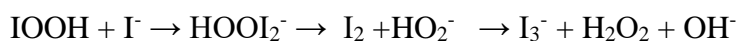
3.4.3. Hydrophilicity of cotton fabrics.

The hydrophilicity of cotton fabric specimens has been measured by a static immersion test. The results showed water absorption of the cotton sample treated with [Cu₂(D)(NO₃)₄] (86%±1.4) to be lower than that of the untreated sample (115%±3.2). That suggests that, when applied onto cotton fabric, the studied dendrimer gains hydrophobic properties, which contribute to the antimicrobial effect of the treated cotton fabric.

3.5. Studies on the behavior of potassium iodide in the presence of [Cu₂(D)(NO₃)₄] and while being deposited on the cotton fabric.

The iodometric method has been used for the production of singlet oxygen (¹O₂) after the irradiation of [Cu₂(D)(NO₃)₄] solutions at a concentration of 1x10⁻⁷ M, as well as from the cotton fabrics dyed with [Cu₂(D)(NO₃)₄] [33-35]. This method is based on the reaction of the singlet oxygen released when irradiating the dendrimers with I⁻ to give I₃⁻ by the following mechanism.





where: $[\text{Cu}_2(\text{D})(\text{NO}_3)_4]_0$, $^1[\text{Cu}_2(\text{D})(\text{NO}_3)_4]$ and $^3[\text{Cu}_2(\text{D})(\text{NO}_3)_4]$ are the metallodendrimer (used as PS) in the ground, singlet and in the triplet excited state.

KI (5ml 0.5 M) solution containing metallodendrimer $[\text{Cu}_2(\text{D})(\text{NO}_3)_4]$ at a concentration of 1×10^{-7} M has been irradiated by a Newport solar simulator: 185-1100 nm, Xe lamp 150 W, at 30 cm sample distance. The absorption spectra of the solution have been recorded in the 250-500 nm spectral range at intervals of 5 minutes. The spectra of photooxidation of I^- to I_3^- , which is caused by the release of singlet oxygen during the irradiation of metallodendrimer $[\text{Cu}_2(\text{D})(\text{NO}_3)_4]$ are plotted in Figure 4. Two well-pronounced maxima at 288 and 352 nm have been registered in the studied spectral region, which is characteristic for I_3^- formed in the solution (Figure 4A). The absorption increases depending on the irradiation time, which can be explained by the increment of the quantity of the singlet oxygen. The same results have been obtained when using cotton fabric treated with $[\text{Cu}_2(\text{D})(\text{NO}_3)_4]$ (Figure 4B). That indicates that the metallodendrimer deposited onto the cotton fabric retains its activity to generate singlet oxygen during the irradiation. Figure 4C compares the absorbance dependence at 352 nm as a function of the irradiation time of $[\text{Cu}_2(\text{D})(\text{NO}_3)_4]$ in solution and after its deposition onto the cotton fabric. As seen, the activity of the dendrimer increases. The irradiated solutions of $[\text{Cu}_2(\text{D})(\text{NO}_3)_4]$ and of cotton dyed fabric without KI have been used as control. No absorption of the solutions has been registered, which evidences the lack of singlet oxygen.

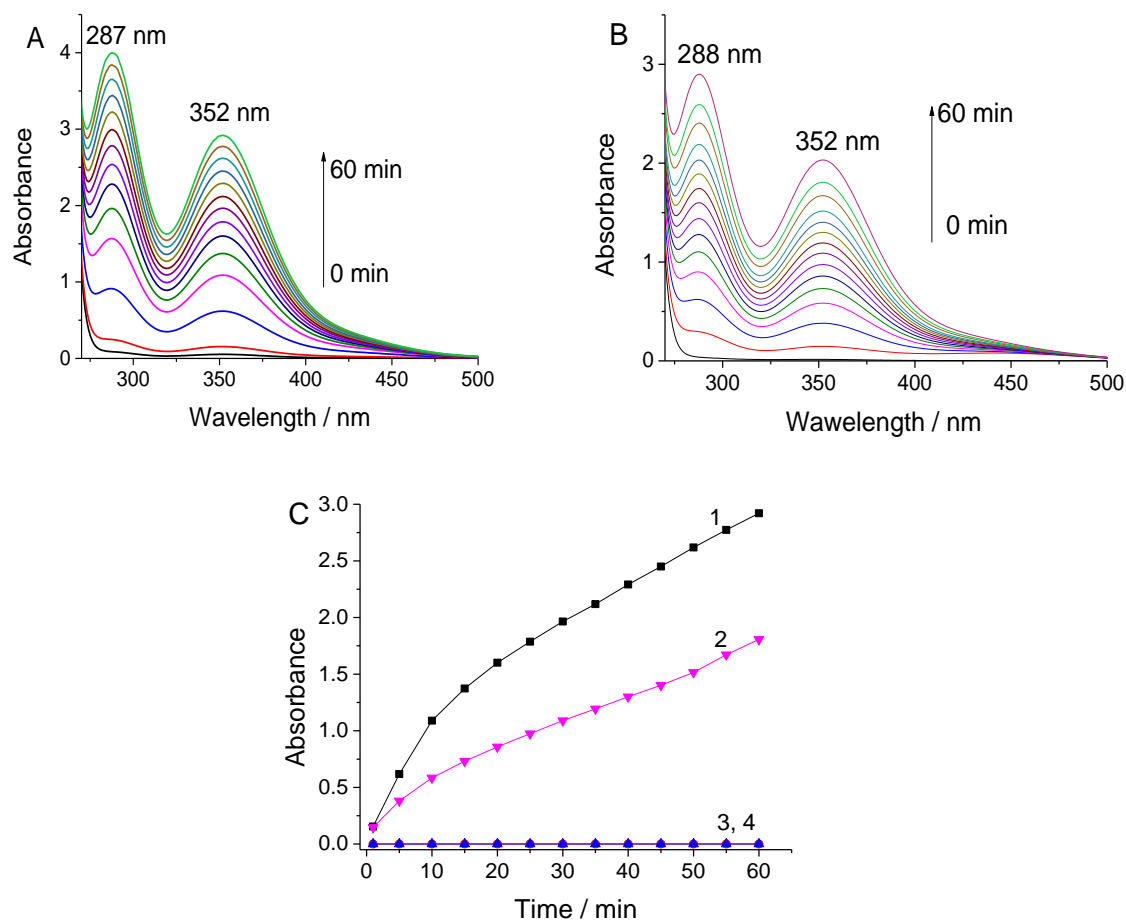


Figure 4. Absorption spectra of KI (0.5M) photooxidated to I_3^- as a function of the irradiation time: (A) in the presence of a 1 cm² cotton fabric dyed with $[\text{Cu}_2(\text{D})(\text{NO}_3)_4]$ and (B) in a solution of $[\text{Cu}_2(\text{D})(\text{NO}_3)_4]$; (C) Dependence of absorbance at 352 nm, corresponding to I_3^- caused by: (1) cotton fabric dyed $[\text{Cu}_2(\text{D})(\text{NO}_3)_4]$, (2) solution of $[\text{Cu}_2(\text{D})(\text{NO}_3)_4]$ comprising: (3) only the dendrimer and (4) only dyed cotton fabrics.

3.6. Cytotoxic activity.

3.6.1. Short-term experiments.

The cytotoxic activity of $[\text{Cu}_2(\text{D})(\text{NO}_3)_4]$ and its ligand D has been examined against the human triple-negative breast cancer cells (permanent cell line MDA-MB-231) after 24 h and 48 h treatment periods. The research has been initiated by an MTT test - the gold standard for cytotoxicity assays. The viability of MDA-MB-23 cells has been monitored at different concentrations of the dendrimers in the 16-133 μM range. The results obtained are plotted in Figure 5A, which shows that metallodendrimer $[\text{Cu}_2(\text{D})(\text{NO}_3)_4]$ has a more pronounced cytotoxic activity compared to that of its ligand. The percent of viable cells has been decreased to 42.2 % ($[\text{Cu}_2(\text{D})(\text{NO}_3)_4]$) and 48.0 % (D) for the first 24 h, as compared to the one caused by the control (Figure 5A). In the next 24 h, the reduction in tumor cells was significant, and around 0.5-1.0% viable cells were found after cultivation in the presence of the compounds examined, which had been administered at a concentration of 133 μM - relative to the tumor cells untreated with the dendrimers (Figure 5B).

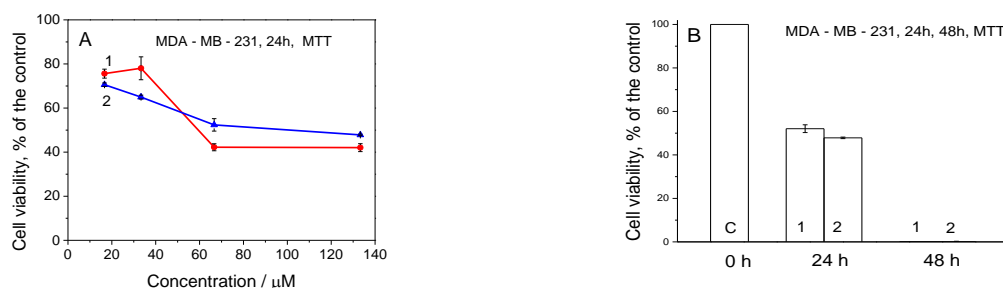


Figure 5. (A) Effect of concentration of dendrimer D (1) and $[\text{Cu}_2(\text{D})(\text{NO}_3)_4]$ (2) on cell viability of MDA-MB-231 human breast cancer cells for 24h. (B) Cell viability at a concentration of both dendrimers 133 μM for 24h and for 48h.

The cytopathological changes in MDA-MB-231 cells induced by dendrimer D and $[\text{Cu}_2(\text{D})(\text{NO}_3)_4]$ at concentrations of 16 μM and 66 μM for 48 h at double staining with acridine orange and propidium iodide have been investigated by fluorescence microscopy, and the results are shown in Figure 6.

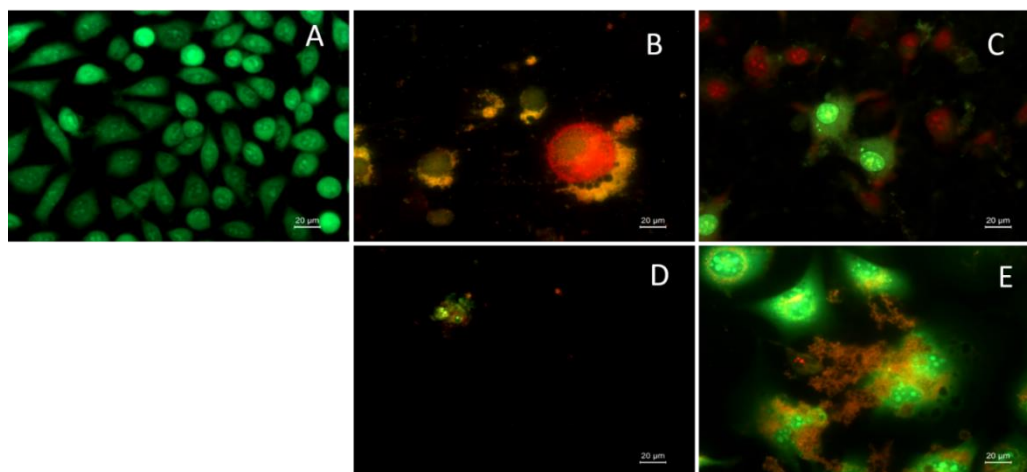


Figure 6. Human triple-negative breast cancer cells (MDA-MB-231 cell line) - (A) culture medium control; (B) culture medium treated for 48 h with 16 μM of $[\text{Cu}_2(\text{D})(\text{NO}_3)_4]$; (C) culture medium treated for 48 h with 16 μM of dendrimer D; (D) culture medium treated for 48 h with 66 μM of $[\text{Cu}_2(\text{D})(\text{NO}_3)_4]$; (E) culture medium treated for 48 h with 66 μM of dendrimer D. Double staining with acridine orange and propidium iodide. (Leica DM 5000B, Leica Microsystems, Germany, 40x). Bar = 20 μm .

A monolayer of vital untreated cells from the MDA-MB-231 line with pale green nuclear fluorescence and bright yellow-green nuclei was used as a control (6A). After 24 h of culturing the cells in the presence of 16 μM $[\text{Cu}_2(\text{D})(\text{NO}_3)_4]$, enlarged dead cells with bright red nuclei of orange color and red fluorescence were observed (6B). During the treatment with dendrimer D, a significant decrease of vital cells was observed simultaneously, with many reduced dead cells stained in orange-red color (6C). With increasing concentration of metallodendrimer (66 μM), single reduced dead cells (6D) were observed, while when treated with dendrimer D, enlarged and rounded fused cells with a large number of red and bright green lysosomal granules were observed (6E).

3.6.2. Long-term experiments.

The effect that the tested dendrimers D and $[\text{Cu}_2(\text{D})(\text{NO}_3)_4]$ have on the anchorage-independent growth of MDA-MB-231 cells has also been evaluated after a 10 day incubation period. The results show that $[\text{Cu}_2(\text{D})(\text{NO}_3)_4]$ completely inhibits 3D growth of human tumor cells at $\geq 33 \mu\text{M}$, while D1 at a concentration of $\geq 66 \mu\text{M}$ reduces the tumor formation.

Table 2. Effect of the dendrimers on the colony-forming ability of human triple-negative breast cancer cells (MDA-MB-231 cell line).

Compound	Concentration, μM	Colony formation, 10 th day
Control		Large colonies > 10 on visual field
$[\text{Cu}_2(\text{D})(\text{NO}_3)_4]$	16	Up to 10 colonies per visual field
	33, 66, 133	Single cells
D	16	No inhibition (> 10 on visual field)
	33, 66	Up to 10 colonies per visual field
	133	Up to 5 colonies per visual field

4. Conclusions

A new metallodendrimer $[\text{Cu}_2(\text{D})(\text{NO}_3)_4]$ based on a PAMAM dendrimer of zero generation modified with 1,8-naphthalimide has been designed, synthesized, and characterized. The new compound underwent studies by IR and EPR spectroscopy for selecting the optimal conditions for its deposition onto cotton fabric. The color characteristics of the dyed textile materials obtained have been determined. Antimicrobial activity of the new metallodendrimer has been studied against Gram-negative bacterium *P. aeruginosa* in the dark and after irradiation with visible light. It has been found that upon irradiation with visible light, the metallodendrimer exhibits more antimicrobial activity than in the dark due to the generation of reactive singlet oxygen. That is an indication that the metallodendrimer investigated has the potential to be used in the design of formulations with antibacterial photodynamic activity. Antitumor activity of the metallodendrimer $[\text{Cu}_2(\text{D})(\text{NO}_3)_4]$ and its ligand D have also been evaluated against human triple-negative breast cancer cells (MDA-MB-231 cell line). The results have revealed that the metallodendrimer possesses an antitumor activity higher than that exhibited by dendrimer D.

Funding

This research received no external funding.

Acknowledgments

The authors acknowledge Grant № KII-06-KOCT/ 4, Fund "Scientific Research", Ministry of Education and Science of Bulgaria.

Conflicts of Interest

The authors declare no conflict of interest.

References

1. Pooresmaeila, M.; Namaz H. Advances in development of the dendrimers having natural saccharides in their structure for efficient and controlled drug delivery applications, *European Polymer Journal* **2021**, *148*, 110356, <https://doi.org/10.1016/j.eurpolymj.2021.110356>.
2. Filipczak, N.; Yalamarty, S.S.K.; Li, X.; Parveen, F.; Torchilin, V. Developments in Treatment Methodologies Using Dendrimers for Infectious Diseases. *Molecules* **2021**, *26*, 3304, <https://doi.org/10.3390/molecules26113304>.
3. Mlynarczyk, D.T.; Dlugaszewska, J.; Kaluzna-Mlynarczyk, A.; Goslinski, T. Dendrimers against fungi – A state of the art review. *J. Control Release* **2021**, *330*, 599–617, <https://doi.org/10.1016/j.jconrel.2020.12.021>.
4. Tarach, P.; Janaszewska, A. Recent Advances in Preclinical Research Using PAMAM Dendrimers for Cancer Gene Therapy. *Int. J. Mol. Sci.* **2021**, *22*, 2912, <https://doi.org/10.3390/ijms22062912>.
5. Staneva, D.; Vasileva-Tonkova, E.; Yordanova, S.; Kukeva, R.; Stoyanova, Grabchev, I. Spectral characterization, antimicrobial and antibiofilm activity of poly (propylene imine) metallodendrimers in solution and applied onto cotton fabric, *Int. J. Polym. Anal. Charact.* **2020**, *25*, 374–384, <https://doi.org/10.1080/1023666X.2020.1796105>.
6. Sanz del Olmo, N.; Carloni, R.; Ortega, P.; García-Gallego, S.; Javier de la Mata, F. Metallodendrimers as a promising tool in the biomedical field: An overview. *Adv. Organomet. Chem.* **2020**, *74*, 1–52, <https://doi.org/10.1016/bs.adomc.2020.03.001>.
7. Mignani, S.; Bignon, J.; Shi, X.; Majoral, J.-P. First-in-Class Phosphorus Dendritic Framework, a Wide Surface Functional Group Palette Bringing Noteworthy Anti-Cancer and Anti-Tuberculosis Activities: What Lessons to Learn? *Molecules* **2021**, *26*, 3708, <https://doi.org/10.3390/molecules26123708>.
8. Alami, O.; Laurent, R.; Majoral, J.-P.; El Brahmi, N.; El Kazzouli, S.; Caminade, A.-M. Copper complexes of phosphorus dendrimers and their properties. *Inorg. Chim. Acta* **2021**, *517*, 120212, <https://doi.org/10.1016/j.ica.2020.120212>.
9. Carloni, R.; Sanz Del Olmo, N.; Canonico, B.; Montanari, M.; Ciacci, C.; Ambrosi, G.; Javier de la Mata, F.; Ottaviani, M.F.; García-Gallego, S. Elaborated study of Cu (II) carbosilane metallodendrimers bearing substituted iminopyridine moieties as antitumor agents. *Eur. J. Med. Chem.* **2021**, *215*, 11392, <https://doi.org/10.1016/j.ejmech.2021.113292>.
10. Sanz del Olmo, N.; Holota, M.; Michlewska, S.; Gómez, R.; Ortega, P.; Ionov, M.; de la Mata, F.J.; Bryszewska, M. Copper (II) Metallodendrimers Combined with Pro-Apoptotic siRNAs as a Promising Strategy Against Breast Cancer Cells. *Pharmaceutics* **2020**, *12*, 727, <https://doi.org/10.3390/pharmaceutics12080727>.
11. Grabchev, I.; Staneva, D.; Betsheva, R. Fluorescent dendrimers as sensors for biologically important metal cation. *Curr. Med. Chem.* **2012**, *29*, 4976–4983, <https://doi.org/10.2174/0929867311209024976>.
12. Staneva, D.; Grabchev, I. Chapter 20 - Dendrimer as antimicrobial agents. *Dendrimer-Based Nanotherapeutics* **2021**, 363–384, <https://doi.org/10.1016/B978-0-12-821250-9.00016-0>.
13. Tutov, M.V.; Sergeev, A.A.; Shamich, N.I.; Chepak, A.K.; Mironenko, Yu.A. Synthesis and optical properties of rhodamine terminated organosilicon dendrimers. *Dyes Pigm.* **2021**, *184*, 108783, <https://doi.org/10.1016/j.dyepig.2020.108783>.
14. Staneva, D.; Grabchev, I. Heterogeneous sensors for ammonia, amines and metal ions based on a dendrimer modified fluorescent viscose fabric. *Dyes Pigm.* **2018**, *155*, 164–170, <https://doi.org/10.1016/j.dyepig.2018.03.044>.
15. Bosch P.; Staneva, D.; Vasileva-Tonkova, E.; Grozdanov, P.; Nikolova, I.; R. Kukeva, R.; Stoyanova, R.; Grabchev, I. New Poly (Propylene Imine) Dendrimer Modified with Acridine and Its Cu (II) Complex: Synthesis, Characterization and Antimicrobial Activity. *Materials* **2019**, *12*, 3020, <https://doi.org/10.3390/ma12183020>.
16. Staneva, D.; Yordanova, S.; Vasileva-Tonkova, E.; Stoyanov, S.; Grabchev, I. Synthesis of a new fluorescent poly (propylene imine) dendrimer modified with 4-nitrobenzofurazan. Sensor and antimicrobial activity. *J. Photochem. Photobiol. A Chemistry* **2020**, *395*, 112506, <https://doi.org/10.1016/j.jphotochem.2020.112506>.

17. Dodangeh, M.; Gharanjig, K.; Tang, R.C.; Grabchev, I. Functionalization of PAMAM dendrimers with curcumin: Synthesis, characterization, fluorescent improvement and application on PET polymer. *Dyes Pigm.* **2020**, *174*, 108081, <https://doi.org/10.1016/j.dyepig.2019.108081>.
18. Staneva, D.; Vasileva-Tonkova, E.; Bosch, P.; Grozdanov, P.; Grabchev, I. Synthesis and characterization of a new PAMAM metallodendrimer for antimicrobial modification of cotton fabric. *Macromol. Res.* **2018**, *26*, 332, <https://doi.org/10.1007/s13233-018-6043-x>.
19. Grabchev, I.; Vasileva-Tonkova, E.; Staneva, D.; Bosch, P.; Kukeva, R.; Stoyanova, R. Impact of Cu (II) and Zn (II) ions on the functional properties of new PAMAM metallodendrimers. *New J. Chem.* **2018**, *42*, 7853–7862, <https://doi.org/10.1039/C8NJ00384J>.
20. Staneva, D.; Vasileva-Tonkova, E.; Grabchev, I. pH sensor potential and antimicrobial activity of a new PPA dendrimer modified with benzantrone fluorophores in solution and on viscose fabric. *J. Photochem. Photobiol. A Chemistry* **2019**, *375*, 24–29, <https://doi.org/10.1016/j.jphotochem.2019.02.004>.
21. Grabchev, I.; Vasileva-Tonkova, E.; Staneva, D.; Bosch, P.; Kukeva, R.; Stoyanova, R. Synthesis, spectral characterization, and *in vitro* antimicrobial activity in liquid medium and applied on cotton fabric of a new PAMAM metallodendrimer. *Int. J. Polym. Anal. Charact.* **2018**, *23*, 45–57, <https://doi.org/10.1080/1023666X.2017.1387025>.
22. Grabchev, I.; Staneva, D.; Vasileva-Tonkova, E.; Alexandrova, R. Surface Functionalization of Cotton Fabric with Fluorescent Dendrimers, Spectral Characterization, Cytotoxicity, Antimicrobial and Antitumor Activity. *Chemosensors* **2019**, *7*, 17, <https://doi.org/10.3390/chemosensors7020017>.
23. Ingrassia, L.; LeFranc, F.; Kiss, R.; Mijatovic, T. Naphthalimides and Azonafides as Promising Anti-Cancer Agents. *Curr. Med. Chem.* **2009**, *16*, 1192–1213, <https://doi.org/10.2174/092986709787846659>.
24. Gong, H.H.; Addla, D.; Lv, J.S.; Zhou, C.H. Heterocyclic naphthalimides as new skeleton structure of compounds with increasingly expanding relational medicinal applications. *Curr. Top. Med. Chem.* **2016**, *16*, 3303–3364, <https://doi.org/10.2174/1568026616666160506145943>.
25. Carretero, G.P.B.; Saraiva, G.K.V.; Rodrigues, M.A.; Kiyota, S.; Bemquerer, M.P.; Chaimovich, H.; Cuccovia, I.M. Naphthalimide-Containing BP100 Leads to Higher Model Membranes Interactions and Antimicrobial Activity. *Biomolecules* **2021**, *11*, 542, <https://doi.org/10.3390/biom11040542>.
26. Rykowski, S.; Gurda-Woźna, D.; Orlicka-Płocka, M.; Fedoruk-Wyszomirska, A.; Giel-Pietraszuk, M.; Wyszko, E.; Kowalczyk, A.; Stączek, P.; Bak, A.; Kiliszek, A.; Rypniewski, W.; Olejniczak, A.B. Design, Synthesis, and Evaluation of Novel 3-Carboranyl-1,8-Naphthalimide Derivatives as Potential Anticancer Agents. *Int. J. Mol. Sci.* **2021**, *22*, 2772, <https://doi.org/10.3390/ijms22052772>.
27. Grabchev, I.; Qian, X.; Bojinov, V.; Xiao, Y.; Zhang, W. Synthesis and Photophysical Properties of 1,8-Naphthalimide Labelled Dendrimers as PET Sensors of Proton and Transition Metal Ion. *Polymer* **2002**, *43*, 5731–5736, [https://doi.org/10.1016/S0032-3861\(02\)00417-2](https://doi.org/10.1016/S0032-3861(02)00417-2).
28. Grabchev, I.; Chovelon, J.-M.; Qian, X. Polyamidoamine Dendrimer with Peripheral 1,8-naphthalimide Groups Capable of Acting as PET Fluorescent Sensor for Metal Cations. *New J. Chem.* **2003**, *27*, 337–340, <https://doi.org/10.1039/B204727F>.
29. Panchenko, P.A.; Fedorova, O.A.; Fedorov, Yu.V. Fluorescent and colorimetric chemosensors for cations based on 1,8-naphthalimide derivatives: design principles and optical signalling mechanisms. *Russ. Chem. Rev.* **2014**, *83*, 155–182, <http://dx.doi.org/10.1070/RC2014v083n02ABEH004380>.
30. Peisach, J.; Blumberg, W.E. Structural implications derived from the analysis of electron paramagnetic resonance spectra of natural and artificial copper proteins. *Arch. Biochem. Biophys.* **1974**, *165*, 691–708, [https://doi.org/10.1016/0003-9861\(74\)90298-7](https://doi.org/10.1016/0003-9861(74)90298-7).
31. Becerir, B. A novel approach for estimating the relation between K/S value and dye uptake in reactive dyeing of cotton fabrics. *Fibers and Polymers* **2005**, *6*, 224–228, <https://doi.org/10.1007/BF02875646>.
32. Sperandio, F.F.; Huang, Y.-Y.; Hamblin, M.R. Antimicrobial Photodynamic Therapy to Kill Gram-negative Bacteria. *Recent Pat. Antiinfect. Drug Discov.* **2013**, *8*, 108–120, <https://doi.org/10.2174/1574891x113089990012>.
33. López-Fernández, A.M.; Muñoz Resta, I.; de Llanos, R.; Galindo, F. Photodynamic Inactivation of *Pseudomonas aeruginosa* by PHEMA Films Loaded with Rose Bengal: Potentiation Effect of Potassium Iodide. *Polymers* **2021**, *13*, 2227, <https://doi.org/10.3390/polym13142227>.
34. Wan, L.; Yiming, X. Iodine-sensitized oxidation of ferrous ions under UV and visible light: the influencing factors and reaction mechanism. *Photochem. Photobiol. Sci.* **2013**, *12*, 2084–2089, <https://doi.org/10.1039/C3PP50245G>.
35. Bartolomeu, M.; Oliveira, C.; Pereira, C.; Neves, M.G.P.M.S.; Faustino, M.A.F.; Almeida, A. Antimicrobial Photodynamic Approach in the Inactivation of Viruses in Wastewater: Influence of Alternative Adjuvants. *Antibiotics* **2021**, *10*, 767, <https://doi.org/10.3390/antibiotics10070767>.

Supporting Information

Spectral measurements

Varian Cary 5000 UV-Vis-NIR Spectrophotometer has been used for UV-vis spectrophotometric measurements. The color coordinates ($L^*a^*b^*$, XYZ and xy) of dyed cotton fabric with dendrimers were determined by Datacolor Spectraflash SF300 spectrophotometer (Datacolor, NJ, USA) and Micromatch 2000® software. Dulbecco's modified Eagle's medium (DMEM) and fetal bovine serum (FBS) were purchased from Gibco-Invitrogen (UK). Dimethyl sulfoxide (DMSO), neutral red, crystal violet, and trypsin were obtained from AppliChem (Germany), thiazolyl blue tetrazolium bromide (MTT), trypan blue and purified agarose were from Sigma-Aldrich Chemie GmbH (Germany). The antibiotics (penicillin and streptomycin) were from Lonza (Belgium).

Antimicrobial assay

The ability of the compound $[\text{Cu}_2(\text{D})(\text{NO}_3)_4]$ to inhibit the growth of Gram-negative strain *Pseudomonas aeruginosa* was tested in meat-peptone broth (MPB) in the presence of light and in the dark. The compound was dissolved in DMSO at a starting concentration of 5 mg/mL and further diluted serially in test tubes with meat-peptone broth (MPB) to final concentrations in the range of 51-306 μM . Two sets of tubes were prepared – for experiments in the presence of light and in the dark. After inoculation with standardized cell suspension, the tubes were incubated at an appropriate temperature for 20 h under shaking. Positive controls (compound and MPB, without inoculum) and negative controls (MPB and inoculum, without compounds) were used. The turbidity of the medium at 600 nm (OD_{600}) was determined as a measure of microbial growth. The lowest concentration of dendrimers that inhibited the growth of the strain by more than 90% was referred to as MIC. The experiments were conducted in triplicate, and the averages were taken (standard deviations less than 5%). The antibacterial effect of cotton fabric treated with 0.25w% solution of $[\text{Cu}_2(\text{D})(\text{NO}_3)_4]$ was tested against *P. aeruginosa* in MPB under light irradiation and in the dark. Test tubes containing MPB and square-shaped cotton specimens (10 mm x 10 mm) were inoculated with standardized microbial suspension. Tubes with native cotton and without specimens were also prepared as controls. Two sets of tubes were prepared for testing in the presence and absence of light. After 20 h incubation at an appropriate temperature, the specimens were removed, and OD_{600} determined microbial growth. The antimicrobial activity of the samples was evaluated by the reduction of bacterial growth in the presence of the treated specimens compared to native. All assays were performed in triplicate, and the averages were taken (standard deviations less than 5%).

Assessment of hydrophilicity of cotton fabrics

The hydrophilicity of the untreated cotton fabric and cotton fabric treated with the new compound $[\text{Cu}_2(\text{D})(\text{NO}_3)_4]$ was assessed using a static immersion test reported in ATCC Technical Manual 2001. In this test, the amount of water absorbed by the fabric was measured. The cotton fabrics were weighed and immersed to a depth of 10 cm in a beaker with distilled water. The cotton fabrics were removed after 5 min and tapped to remove the excess water, and then weighed once again. The absorption was determined by the following formula: Absorption (%) = (mass of water absorbed/original mass) \times 100

EPR structural investigations of [Cu₂(D)(NO₃)₄]

The EPR spectra of complexes were recorded using a Bruker EMXplus EPR spectrometer working in the X-band (9.4 GHz) and temperature range of 120–450 K. The spectra simulation was accomplished within the software SIMFONIA (Bruker).

Cell cultures and cultivation

The human permanent cell line established from triple-negative breast cancer MDA-MB-231 was used as a model system in the study. The cells do not express estrogen receptors either receptors for progesterone and HER-2/Neu receptors; they possess mutant p53 gene.

The cells have been grown as a monolayer culture in DMEM medium supplemented in the presence of 10% fetal bovine serum, 100 U/mL penicillin, and 100 µg/mL streptomycin. Thermo Scientific, HEPA Class 100) at 37 °C under 5% CO₂ in the air. For routine passages, the cells were detached using a mixture of 0.05% trypsin and 0.02% ethylenediaminetetraacetic acid (EDTA). The cell line was passaged 2–3 times per week (1:2 to 1:3 split).

Cytotoxicity assays

The cells were seeded in 96-well flat-bottom microplates for cell culturing at a concentration of 1×10^4 cells/well. After the cells were grown for 24 h to a sub-confluent state (~70%), the culture medium was removed and changed by media modified with different concentrations of the compounds tested. Each concentration was applied into 4–8 wells.

The effect of the compounds on cell viability/proliferation was assessed using MTT test after 24 h, 48 h, and 72 h of incubation, neutral red uptake cytotoxicity assay (NR), crystal violet staining (CV), and trypan blue dye exclusion test (TB) after 72 h of incubation.

The cell viability assay was performed by incubating the cells for 3 hours with a solution of 5 mg MTT in 10 mL DMEM) at 37 °C and 5% CO₂. The blue MTT formazan has been separated by extraction from ethanol and DMSO in a volume ratio of 1: 1.

Cell viability is expressed as a percentage of the control and the corresponding curves depending on the concentration of the compounds were constructed. On this basis, the CC50 and / or CC90 values are also calculated where possible.

Cytopathological changes

The ability of compounds to induce cytopathological changes was assessed using double staining with acridine orange and propidium iodide (PI) as it was earlier described (Alexandrova et al., 2012). The cells were grown on coverslips ($3.0\text{--}3.5 \times 10^5$ cells/well) in 6-well plates in the presence of the tested compounds. Non-treated cells have been used as control. After 72 h of incubation, the coverslips were removed and washed with PBS for 2 min. Equal volumes of 10 mg/mL in PBS acridine orange and 10 mg/mL in bi-distilled water propidium iodide were added to the cells. The stained cells thus obtained were placed on a glass slide and examined by a fluorescence microscope (Leica DM 500B, Wetzlar, Germany).

3D cell colony-forming method

Tumor cells (10^3 cells/well) suspended in 0.45% agarose and D-MEM medium containing different concentrations of the compounds examined as well as culture medium control were layered in 24 well microplates. The presence/absence of colonies was registered

using an inverted light microscope (Carl Zeiss, Germany) during a period of 20–32 days. Colony inhibitory concentration (CIC, μM) at which the compounds tested completely inhibited the 3D growth of tumor cells in a semi-solid medium was determined. The number of 3D cell colonies was counted in 3–5 independent fields for each compound/concentration.

Statistical analysis

Significant differences between experimental groups and control groups were evaluated by ANOVA followed by Dunnett's posthoc analysis. GraphPad Prism, GraphPadSoftware Inc., USA, 2000. The effective concentrations of the compounds CC_{50} and/or CC_{90} were estimated by Origin 6.1TM.